

Supporting Information

Chiral helix amplification and enhanced bioadhesion of two-component low molecular weight hydrogels regulated by OH to eradicate MRSA biofilm

Zhijia Wang ^{a†}, Tong Li ^{b†}, Xuemei Huang ^{a†}, Ran Xu ^a, Yihang Zhao ^a, Jichang Wei ^a,
Wenmin Pi ^a, Shuchang Yao ^a, Jihui Lu^a, Xiang Zhang ^a, Haimin Lei ^a, Penglong Wang ^{a*}

[a] School of Chinese Pharmacy, Beijing University of Chinese Medicine,
Beijing 102488, China

[b] Chinese Institute for Brain Research, Beijing, 102206, China
E-mail: wpl581@126.com

Table of Contents

1. Experimental Section
 - 1.1 Materials
 - 1.2 Experimental Method
2. Results and Discussion
 - 2.1 Supplementary Figures
 - 2.2 Supplementary Tables
3. References

1. Experimental Procedures

1.1 Materials

Berberine (BBR) and baicalin (BA) and scutellarin (SCU) were purchased from Beijing Inokai Technology Co., Ltd. *Staphylococcus aureus* (ATCC 43300) were purchased from Ningbo Mingzhou Biotechnology Co., Ltd.

1.2 Experimental Method

Preparation and basic properties of BA-BBR hydrogel and SCU-BBR hydrogel: The gel formation process consists of two steps: Step 1: Add a base (NaOH) to dissolve BA and SCU in water. Step 2: Mix the aqueous solutions of BA and SCU with the aqueous solution of BBR hydrochloride at a 1:1 ratio. After cooling to room temperature, the binary system transforms into a transparent hydrogel, which is confirmed using the inverted test tube method.

FESEM analysis of self-assembly: We first shake out and disperse the obtained hydrogel with deionized water and then absorb 10 μ L sample onto the silicon wafer. The samples were dried in vacuum at room temperature, subsequently coated with gold film using a LEICA-EM-ACE600 sputter coater instrument (Leica, Germany). Finally, the morphology of the self-assembly was imaged on a FESEM (ZEISS-SUPRA55, Germany) operated at 8 kV.

ESI-MS spectrum: ESI-MS was tested on a Static Spray-HRMS (Waters, US). The test results were carried out in the negative ion mode. For valuable quasi-molecular ion peaks, Secondary Mass Spectrometry of them were further determined.

Circular Dichroism (CD) spectra: We prepared the 0.25 mM BBR, BA and SCU sodium salt aqueous solution, as well as diluted aqueous solutions of BA-BBR and SCU-BBR hydrogels at different pH (3, 4, 5, 6, 7, 8, 9, 10), respectively. CD spectra

was obtained using JASCO J-1500 CD spectrometer. CD spectra of hydrogels were recorded in the UV-vis region (200–400 nm) using a 0.1 mm quartz cuvette.

Ultraviolet-Visible spectroscopy (UV): Sample solutions were prepared as described in CD method. The UV spectra of samples were determined using a UV-visible spectrophotometer (HITACHI UH5300, Japan) with the scanning range from 200 to 500 nm.

Fourier transform infrared spectroscopy (FT-IR): The fourier transform infrared spectrometer (Nicolet iS10, Thermo, US) was used to obtain the IR spectra in the range from 4000 to 400 cm^{-1} by using of the KBr method. We compared the lyophilized powder of SCU-BBR hydrogel and their monomers.

Fluorescence emission spectrum: Steady-state fluorescence spectra of self-assemblies were measured on a LS-45 fluorescence spectrophotometer (PerkinElmer, UK) in the range from 450 to 650 nm, with a slit width of 5 nm for both excitation and emission. For the fluorescence emission spectra, the excitation wavelength was set at 350 nm, which is the maximum excitation wavelength of BBR. The scanning rate was set at 80 nm/min. All tests were carried out at 25 °C. All spectra were run on air equilibrated solutions. Sample solutions were prepared as described in UV method.

X-ray powder diffraction measurements: XRD were performed at 40 kV, 40 mA on a Rigku Ultima IV diffractometer using Cu-K α radiation over 2θ range of 5°-50° at room temperature. We compared the lyophilized powder of SCU-BBR at different pH.

Proton nuclear magnetic resonance spectroscopy of $^1\text{H-NMR}$: $^1\text{H-NMR}$ spectra was recorded on an Avance IIIHD 400 MHz spectrometer (Bruker, America) with tetramethylsilane as an internal standard. Monomer components (10 mg) and lyophilized powder of self-assemblies (15 mg) were dissolved by 1 mL DMSO- d_6 .

Chemical shifts δ were given in ppm and coupling constants J in Hz. The $^1\text{H-NMR}$ of self-assemblies were analyzed by referring the $^1\text{H-NMR}$ of monomer compounds.

BA $^1\text{HNMR}$ (400 MHz, $\text{DMSO-}d_6$): δ (ppm) 6.94 (s, 1H, H-3), 6.99 (s, 1H, H-8), 8.01 (d, $J = 6.6$ Hz, 2H, H-2', 6'), 7.54-7.53 (m, 3H, H-3', 4', 5'), 12.53 (s, 1H, 5-OH), 8.61 (s, 1H, 6-OH), 5.19 (d, $J = 7.0$ Hz, 1H, BA H-1''), 3.30-3.40 (m, 3H, H-2'', 3'', 4''), 4.01 (d, $J = 9.4$ Hz, 1H, H-5'').

SCU $^1\text{HNMR}$ (400 MHz, $\text{DMSO-}d_6$): δ (ppm) 6.82 (s, 1H, H-3), 7.00 (s, 1H, H-8), 7.94 (d, $J = 7.9$ Hz, 2H, H-2', 6'), 6.95 (d, $J = 7.9$ Hz, 2H, H-3', 5'), 12.75 (s, 1H, 5-OH), 8.61 (s, 1H, 6-OH), 10.38 (s, 1H, 4'-OH), 5.23 (d, $J = 7.1$ Hz, 1H, H-1''), 3.36-3.47 (m, 3H, H-2'', 3'', 4''), 4.06 (d, $J = 9.4$ Hz, 1H, H-5'').

BBR $^1\text{H NMR}$ (400 MHz, $\text{DMSO-}d_6$): δ (ppm) 7.80 (s, 1H, H-1), 7.09 (s, 1H, H-4), 3.21 (brs, 2H, 5- CH_2 -), 4.96 (brs, 2H, 6- CH_2 -), 9.92 (s, 1H, H-8), 8.20 (d, $J = 8.0$ Hz, 1H, H-11), 8.01 (d, $J = 8.0$ Hz, 1H, H-12), 8.98 (s, 1H, H-13), 6.18 (s, 2H, 15- CH_2 -), 4.10 (s, 3H, 9- OCH_3), 4.07 (s, 3H, 10- OCH_3).

BA-BBR hydrogel $^1\text{HNMR}$ (400 MHz, $\text{DMSO-}d_6$): δ (ppm) 6.93 (overlap, 2H, H-3, 8, BA), 8.03 (d, $J = 7.2$ Hz, 1H, H-2', 6', BA), 7.55-7.62 (m, 3H, H-3', 4', 5', BA), 4.97 (d, $J = 5.1$ Hz, 1H, H-1'', BA), 3.23-3.36 (m, 3H, H-2'', 3'', 4'', BA), 3.60 (d, $J = 9.6$ Hz, 1H, H-5'', BA), 7.74 (s, 1H, H-1, BBR), 7.02 (s, 1H, H-4, BBR), 3.19 (m, 2H, 5- CH_2 -, BBR), 4.93 (m, 2H, 6- CH_2 -, BBR), 9.94 (s, 1H, H-8, BBR), 8.08 (d, $J = 9.0$ Hz, 1H, H-11, BBR), 7.93 (d, $J = 9.0$ Hz, 1H, H-12, BBR), 8.90 (s, 1H, H-13, BBR), 6.14 (s, 2H, 15- CH_2 -, BBR), 4.07 (s, 3H, 9- OCH_3 , BBR), 3.97 (s, 3H, 10- OCH_3 , BBR).

SCU-BBR hydrogel $^1\text{HNMR}$ (400 MHz, $\text{DMSO-}d_6$): δ (ppm) 6.81 (s, 1H, H-8, SCU), 6.99 (s, 1H, H-4, BBR), 7.75 (d, $J = 7.4$ Hz, 2H, H-2', 6', SCU), 6.86 (d, $J = 8.3$ Hz, 2H, H-3', 5', SCU), 4.97 (d, $J = 4.0$ Hz, 1H, H-1'', SCU), 3.29-3.34 (m, 3H, H-2'', 3'', 4'', SCU), 3.70 (d, $J = 8.9$ Hz, 1H, H-5'', SCU), 7.70 (s, 1H, H-1, BBR), 6.62 (s, 1H, H-3, SCU), 3.17 (brs, 2H, 5- CH_2 -, BBR), 4.91 (brs, 2H, 6- CH_2 -, BBR), 9.91 (s, 1H,

H-8, BBR), 8.02 (d, $J = 6.2$ Hz, 1H, H-11, BBR), 7.89 (d, $J = 6.2$ Hz, 1H, H-12, BBR), 8.84 (s, 1H, H-13, BBR), 6.13 (s, 2H, 15-CH₂-, BBR), 4.05 (s, 3H, 9-OCH₃, BBR), 3.94 (s, 3H, 10-OCH₃, BBR).

ROESY 2D NMR spectrum: ROESY 2D NMR spectrum was used to detect intermolecular nuclear overhauser effects of self-assemblies. The ROESY 2D spectrum was collected with mixing time of 500 ms under the spin lock condition using Avance IIIHD 700 MHz Spectrometer (Bruker, America).

Biofilm quantitative assay: Preparation of XTT solution: Weigh 5 mg of XTT and dissolve it in PBS to prepare a solution with a concentration of 0.5 mg/mL, then filter it using a microporous filter. Weigh 5 mg of vitamin K and dissolve it in acetone to prepare a solution with a concentration of 0.4 mM. Add 10 μ L of the vitamin K solution to the XTT solution and mix thoroughly to achieve a final concentration of 1 μ M. Prepare this mixture fresh before use and store it protected from light.

Administration and Biofilm Removal Rate Detection: First, inject a high-glucose bacterial culture with a concentration of 2×10^4 CFU/mL into a 96-well plate using a pipette. After incubating at 37°C for 24 hours, remove the culture medium. You will observe biofilm attachment at the bottom of the 96-well plate. Then, add BBR solutions at concentrations of 0.1 μ mol/mL, 0.2 μ mol/mL, 0.4 μ mol/mL, and 0.8 μ mol/mL, as well as BA-BBR hydrogel and SCU-BBR hydrogel. Continue incubating at 37°C for another 24 hours. Next, remove the supernatant and wash the wells three times with PBS buffer. Add 100 μ L of XTT solution to each well and incubate at 37°C for 2 hours. Measure the absorbance at a wavelength of 490 nm. Use the blank culture medium as the solvent control and the culture medium with bacteria as the blank bacterial control. Calculate the biofilm removal rate using the following formula:

$$\text{Removal Rate (\%)} = 100 - \left[\frac{(\text{OD}_{\text{sample}} - \text{OD}_{\text{solvent}})}{(\text{OD}_{\text{blank bacteria}} - \text{OD}_{\text{solvent}})} \right] \times 100\%$$

Optical microscopic observation: The coverage of hydrogel on biofilm surface were observed under a Nikon inverted microscope ECLIPSE Ts2R (Japan). The co-cultivation method of the biofilm and the samples has been described above.

Visual assay of the ability of the sample to remove biofilm by SEM: In order to observe the biofilm by SEM, the above bacterial inoculum was cultured on equal size silicon wafers (0.5 cm × 0.5 cm) for 24 h at 37 °C. After 24h administration of samples, the bacteria were washed with PBS and fixed in 2.5% glutaraldehyde at 37 °C for 4 h, followed by one washing step with PBS. The samples were then dehydrated with increasing concentrations of ethanol (30, 50, 70, 80, 90, 95, and 100%) for 10 min. After being dried in air at room temperature and coated by gold sputter, the samples were examined with a FESEM (ZEISS-SUPRA55, ZEISS, Germany).

The details of calculation in quantum chemistry and molecular dynamic stimulation : The computational methods in this study predominantly involve molecular dynamics (MD) simulations and quantum chemistry calculations based on density functional theory (DFT). Initially, molecular structure models for Baicalin (BA), Scutellarin (SC), Berberine (BBR), and N-Acetyl-Glucosamine were pre-optimized via GFN2-xTB. ^[1] These structures were further refined and subjected to vibrational analysis using ORCA 5.0.3 ^[2] with the B97-3C ^[3] functional. All optimized configurations were verified to have no imaginary frequencies. The resulting wave functions were then analyzed using Multiwfn ^[4] to obtain RESP charges. ^[5] Subsequently, the optimized molecular structures were used to derive force field parameters for molecular dynamics simulations using the GAFF ^[6] force field and the calculated RESP charges. An initial simulation box with a side length of 6 nm, containing 200 N-Acetyl-Glucosamine molecules, was constructed and solvated using the TIP3P ^[7] water model. Molecular dynamics simulations were then performed using Gromacs 2020.6 ^[8], starting with 50,000 steps of energy minimization using the conjugate gradient method. This was followed by a 200 ps NPT ensemble equilibration, during which the temperature was gradually increased from 0 K to 298.15 K over the

first 100 ps. Finally, a 200 ns NPT ensemble production run was conducted at 298.15 K and 1 atm pressure. The stable structure from the last frame of the simulation was used as the initial model for further simulations, where either BA-BBR or SC-BBR complexes were inserted at specific proportions. This was followed by additional energy minimization, a 200 ps equilibration, and a 70 ns production MD simulation. Visual analysis of the MD simulations was performed using VMD [9], and various properties such as the number of hydrogen bonds, solvent-accessible surface area, and root mean square deviation were analyzed using Gromacs tools like hbond, sasa, and rms.

Hemolytic Rate Test: Hemolytic assay of the hydrogel was done using fresh rat blood. We centrifuged the blood at 3000 rpm for 15 min and collected the red blood cells (RBCs). Normal saline was used to rinse RBCs three times. Then we mixed 3 mL of centrifuged RBCs into 11 mL of normal saline as the storage dispersion for use. The hydrogel were diluted with normal saline at different concentrations (2× MIC, 4 ×MIC, 8× MIC, 16× MIC). Subsequently, we mixed hydrogel dispersion (1 mL) with the storage dispersion (100 µL) to obtain 4% RBC solution. The medium were then cultured at 37 °C for 4 h. Determination of absorbance of the medium at 570 nm by a microplate reader occurred after centrifugation at 3000 rpm for 15 min. The positive control was water, and the negative control was normal saline. The hemolytic rates (RHR%) of hydrogel were calculated according to the following formula: $RHR (\%) = (A_{\text{sample}} - A_{\text{saline}}) / (A_{\text{water}} - A_{\text{saline}}) \times 100\%$

Cytotoxicity test: HACAT cells were treated with hydrogels of different concentrations for 24 h. After culture, 100 µL of culture medium and CCK8 mixed solution were added to the HACAT cells in the 96-well plate and cultured in a constant-temperature incubator for 2 h. Finally, DMSO was added and the absorbance value was measured at 490 nm. Cell survival rate is calculated according to the following formula.

$$\text{Cell survival rate (\%)} = (\text{OD}_{\text{administration}} - \text{OD}_{\text{blank}}) / (\text{OD}_{\text{normal}} - \text{OD}_{\text{blank}}) \times 100\%.$$

Skin sensitization Assessment : C57BL/6 mice (~20 g) were taken from Beijing Vital River Laboratory Animal Technology Company Limited, Beijing, China. The animals were divided into control and test groups. Each mice from both groups had its fur clipped on the back prior to the test. The hydrogel ($10\mu\text{mol}\cdot\text{mL}^{-1}$, 200MIC) and 0.9% NaCl saline (the negative control) were applied topically on the clipped dorsal region of each mice, and covered by a gauze patch secured with occlusive dressing. After 24 hours of exposure, the gauze patch with dressing was removed, and the residual test material was washed away with water. The skin was carefully dried. Observation was made at 24, 48, 72 hours after exposure. Description and grading of the skin reactions for the erythema formation were conducted according to the Magnusson and Kligman grading scale. The percentage of the mice showing Magnusson and Kligman grades of 0, demonstrating that no skin sensitization was produced on mice.

Statistical Analysis: The statistical analysis was performed by SPSS software (Version 20.0) to analyze the variance. All data are expressed as means \pm SD. Differences between groups were examined with independent-sample t test. A p-value of less than 0.05 was considered significant.

2.Results and Discussion

2.1 Supplementary Figures

The hydrogel exhibits both pH-sensitive properties. We separately prepared 10 mM sodium aqueous solutions of BA and SCU at different pH levels. Following the same steps as previously described, the formation of gels in the BA-BBR and SCU-BBR systems was confirmed using the inverted test tube method. Hydrogels can form

in the pH range of 7-10 and are destroyed when $\text{pH} < 7$ or $\text{pH} > 10$.

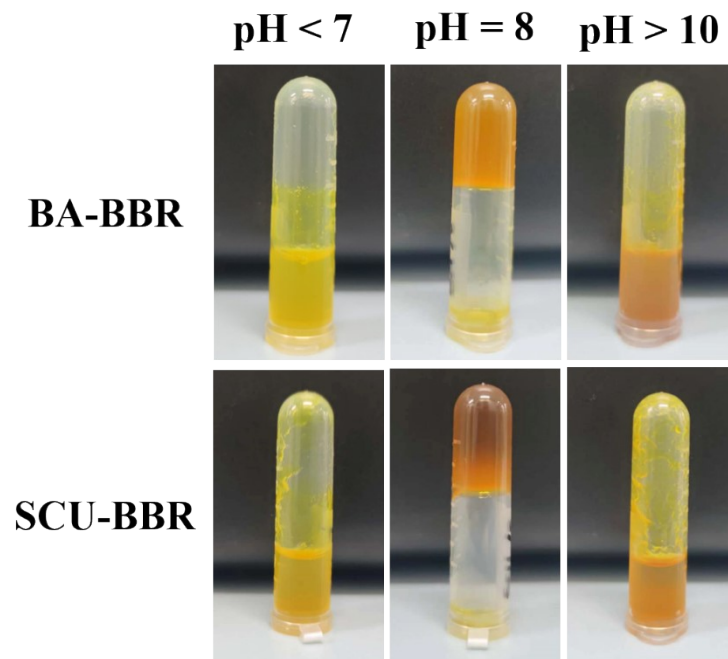


Fig. S1 The status of BA-BBR hydrogel and SCU-BBR hydrogel at different pH

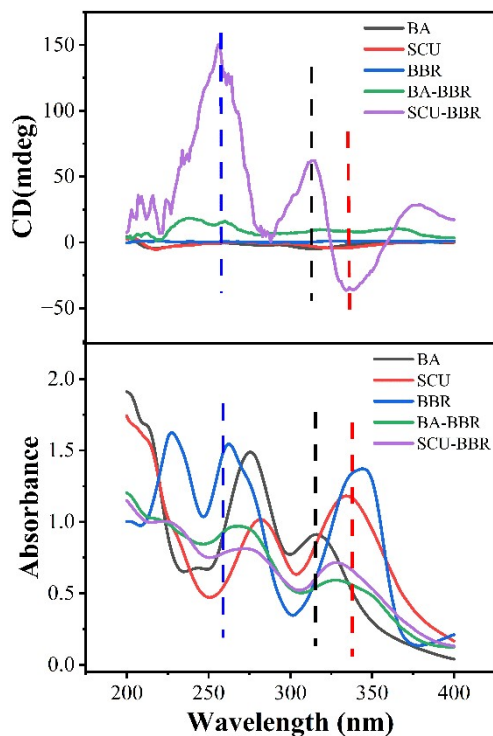


Fig. S2 CD spectra and UV spectra of monomer molecules and BA-BBR hydrogel and SCU-BBR hydrogel.

As shown in Fig. S3, the storage modulus of SCU-BBR hydrogels remains stable at 3300 Pa, whereas that of BA-BBR hydrogels is at 1300 Pa. The storage modulus of SCU-BBR hydrogels is nearly 2.5 times that of BA-BBR hydrogels, indicating that SCU-BBR hydrogels possess superior stability.

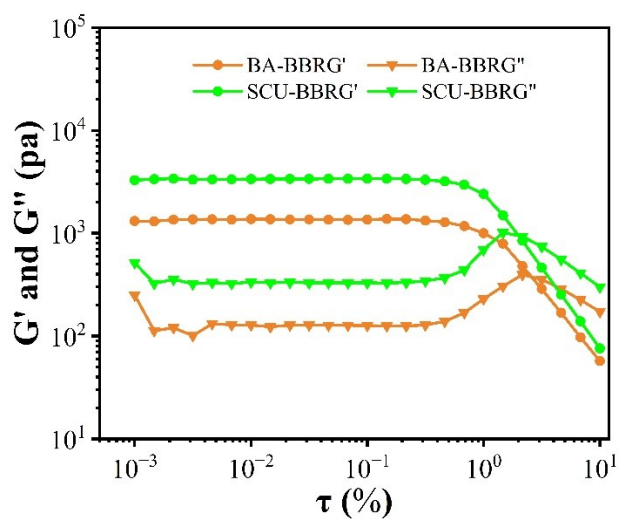


Fig. S3 Changes in G' and G'' of BA-BBR hydrogel and SCU-BBR hydrogel with shear strain.

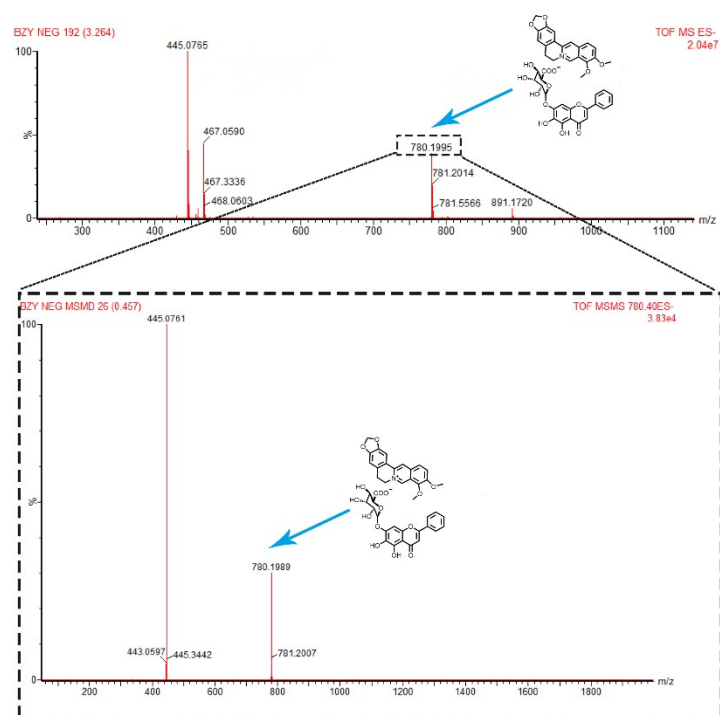


Fig. S4 Molecular weight of a binary unit in ESI-MS spectrum of BA-BBR hydrogel.

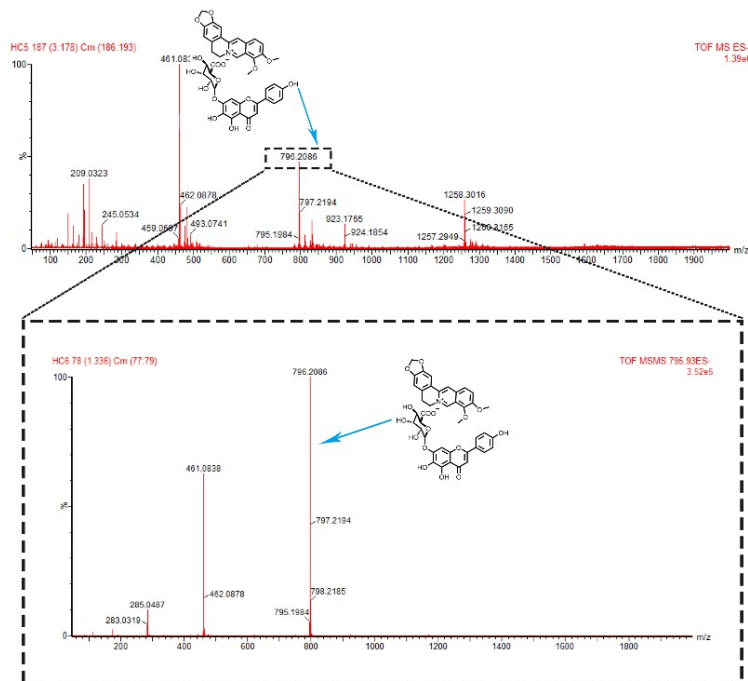


Fig. S5 Molecular weight of a binary unit in ESI-MS spectrum of SCU-BBR hydrogel.

In hydrogel, this peak of the stretching vibration of carbonyl group on glucuronic acid of BA and SCU was shifted to much lower wave number (1726 cm^{-1} to 1615 cm^{-1} for BA, 1720 cm^{-1} to 1604 cm^{-1} for SCU). This was likely due to the formation of a salt bridge between the carboxyl group and the quaternary ammonium ion, which weakens the bond strength of the carboxyl group and reduces the stretching vibration frequency of C=O.

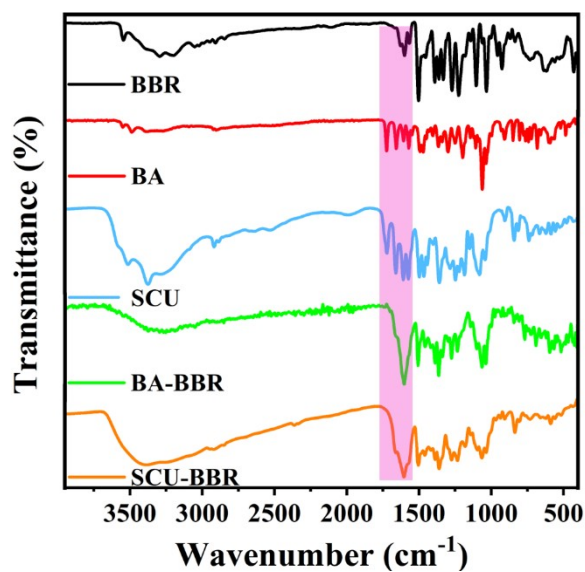


Fig. S6 FT-IR of monomer and hydrogels.

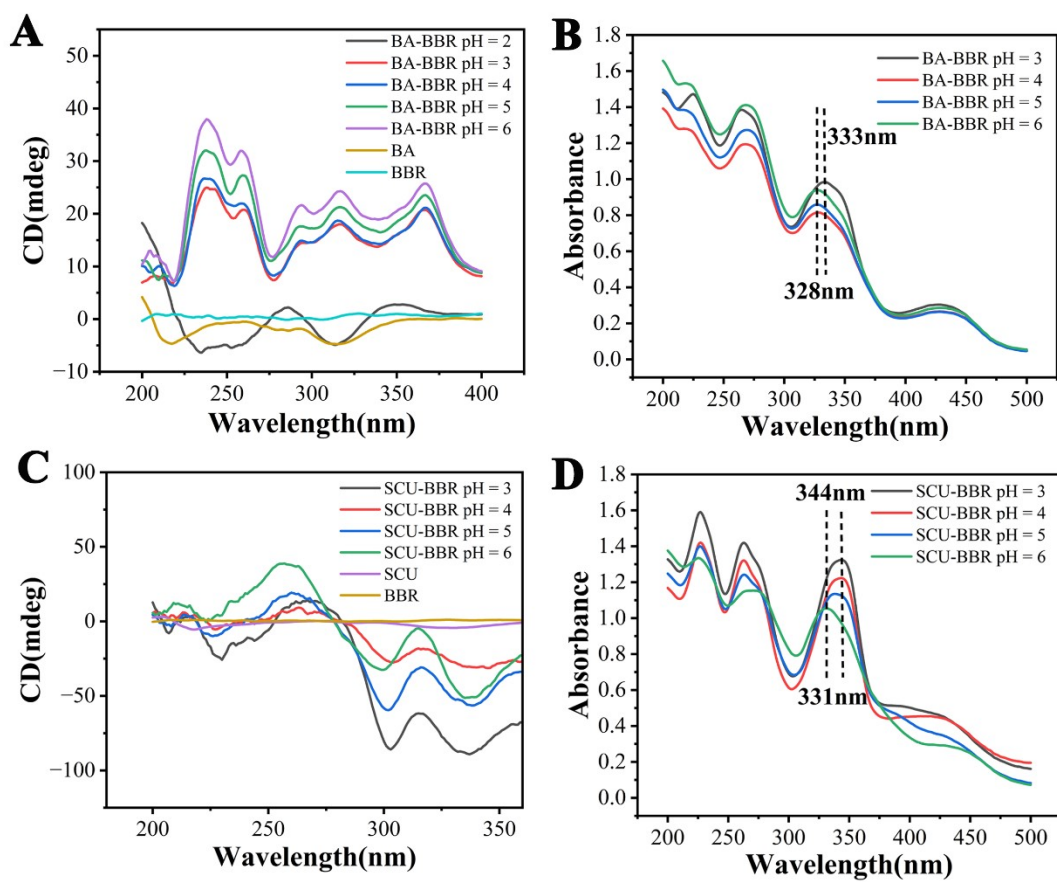


Fig. S7 (A) CD spectra of BA-BBR at different acidic. (B) UV spectra of BA-BBR at different acidic. (C) CD spectra of SCU-BBR at different acidic. (D) UV spectra of SCU-BBR at different acidic.

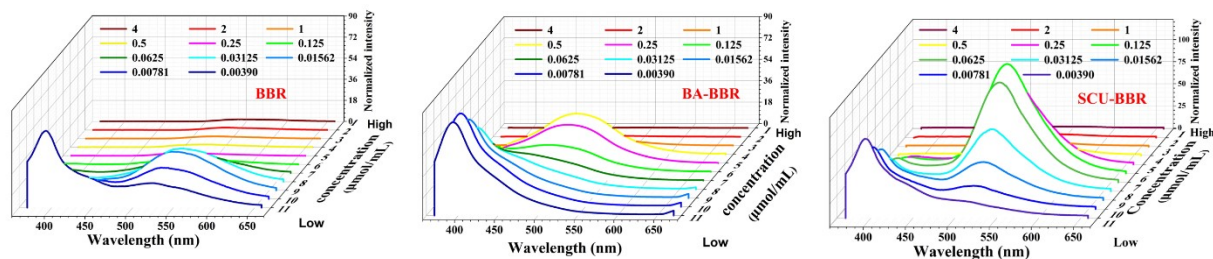


Fig. S8 Fluorescence Emission Spectrum of SCU, BBR and SCU-BBR at different concentration. concentration gradient (4, 2, 1, 0.5, 0.25, 0.125, 0.0625, 0.03125, 0.01562, 0.00781, 0.00390 μmol/mL).

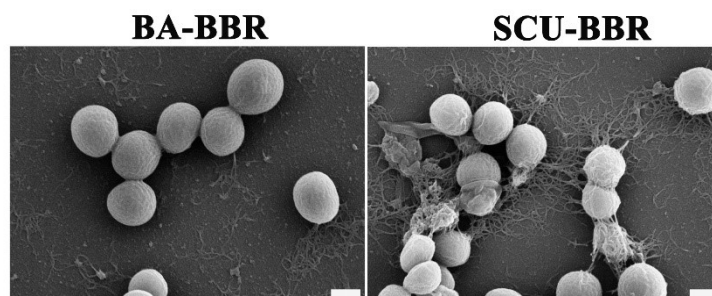


Fig. S9 In SCU-BBR hydrogel group, a large number of nanofibers wind around the bacteria, causing the bacteria to shrink and rupture (scale = 400nm).

BA-BBR

SCU-BBR

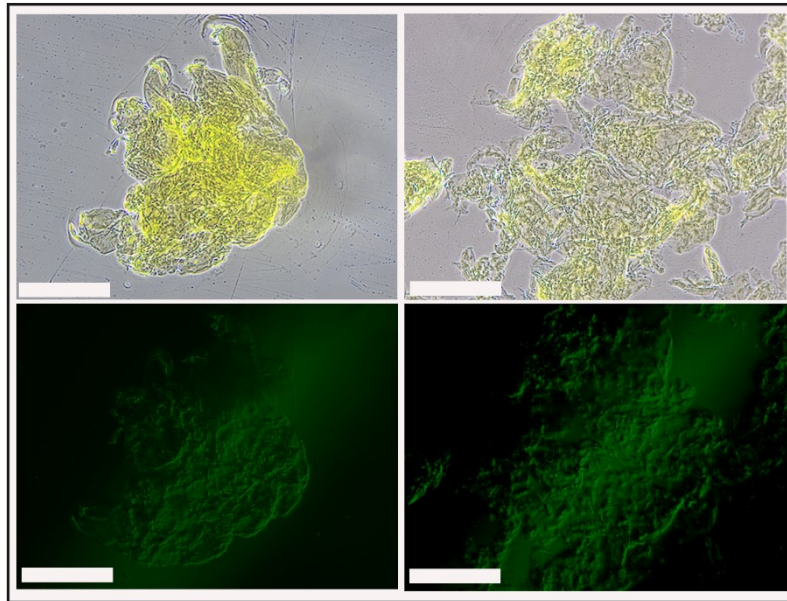


Fig. S10 Fluorescence inverted microscope images of BA-BBR and SCU-BBR (scale = 200 μ m).

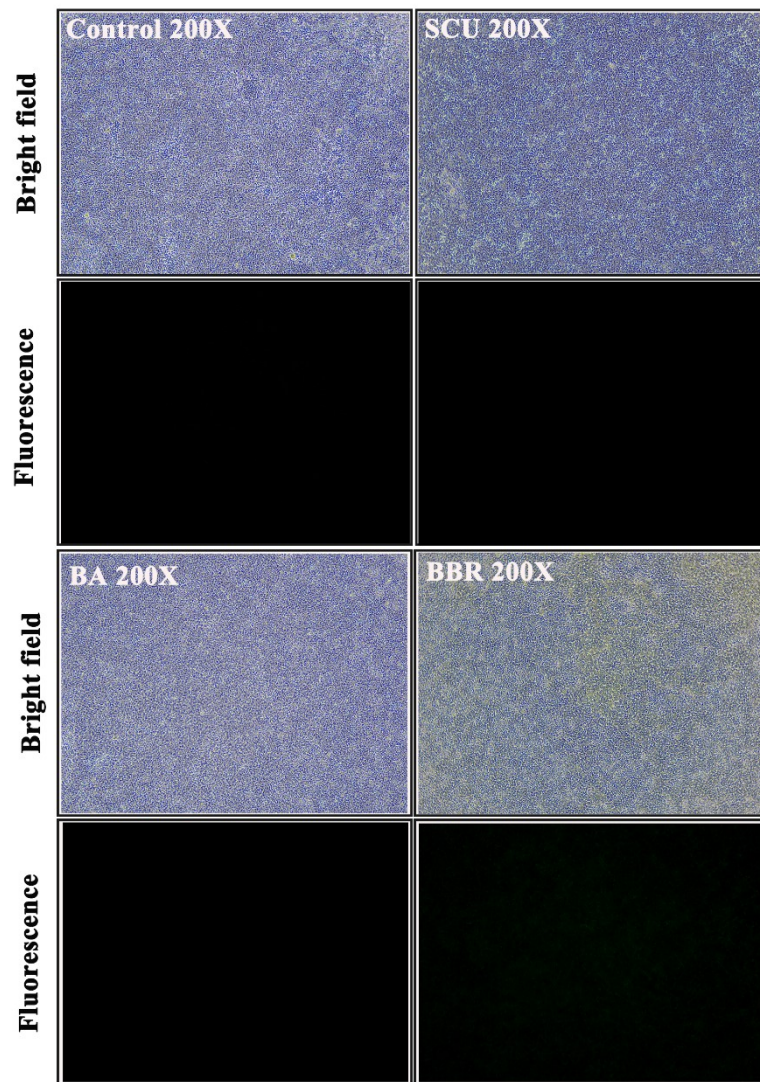


Fig. S11 Fluorescence inverted microscope observed that drug monomer adhered to the biofilm 24 hours after administration.

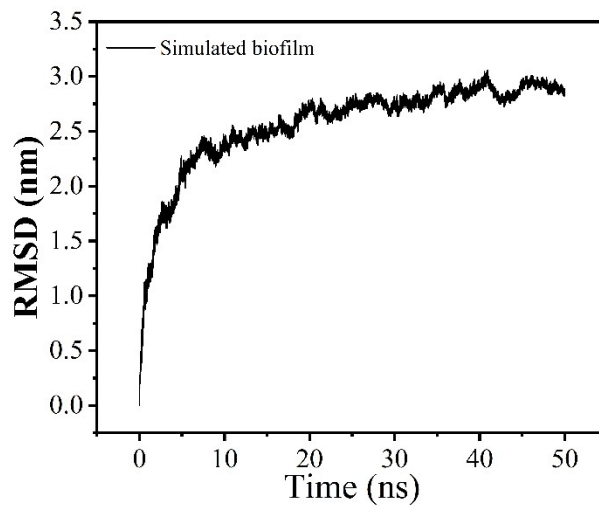


Fig. S12 RMSD of simulated biofilm.

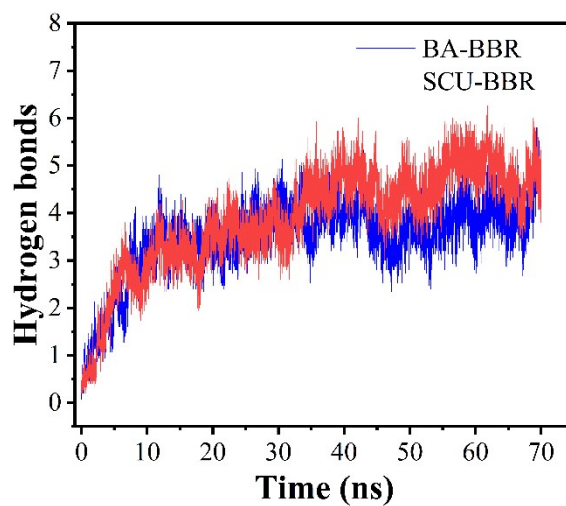


Fig. S13 Hydrogen bonds between the composite units of BA-BBR and SCU-BBR and the biofilm in 70ns molecular dynamics simulation.

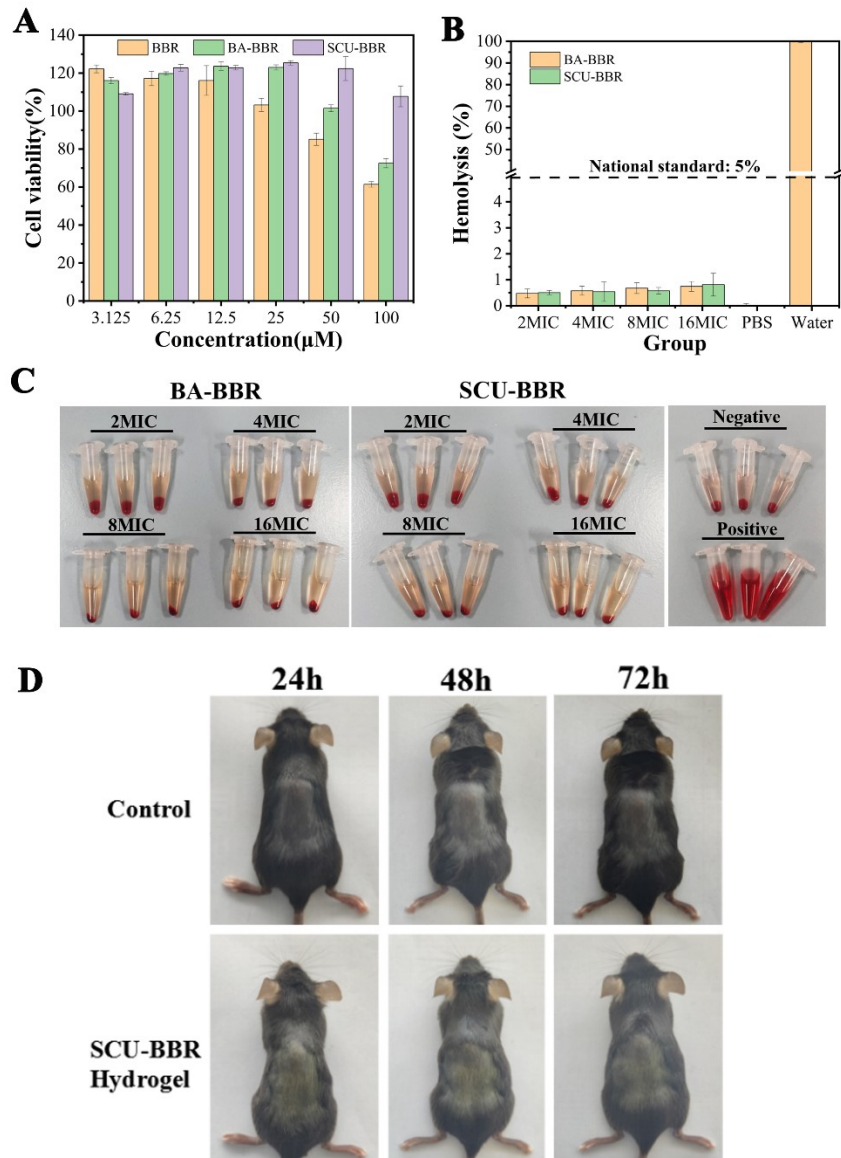


Fig. S14 Biocompatibility of the BA-BBR gel and SCU-BBR gel. (A) Cell viability treated with BBR, BA-BBR gel and SCU-BBR gel at 24 h (n = 3). (B), (C) The hemolytic test of BA-BBR gel and SCU-BBR gel at different concentrations. (D) Skin sensitization assessment of SCU-BBR hydrogel.

2.2 Supplementary Tables

Table S1. Chemical shift changes in ^1H -NMR spectra of BA or SCU during self-assembly.

Position (ppm)	BA-BBR $\Delta\delta$	SCU-BBR $\Delta\delta$
H-1''	-0.22	-0.26
H-5''	-0.41	-0.36
H-2', 6'	-0.03	-0.19
H-3', 5'	-0.03	-0.09
H-3	/	-0.20
H-8	-0.06	-0.19

Table S2. Chemical shift changes in ^1H -NMR spectra of BBR during self-assembly.

Position (ppm)	BA-BBR $\Delta\delta$	SCU-BBR $\Delta\delta$
H-1	-0.06	-0.10
H-4	-0.07	-0.10
H-11	-0.12	-0.18
H-12	-0.08	-0.12
H-13	-0.08	-0.14
10-OCH ₃	-0.10	-0.13
9-OCH ₃	-0.03	-0.05

3 References

- [1] C. Bannwarth, S. Ehlert, S. Grimme, *Journal of Chemical Theory and Computation* **2019**, *15*, 1652-1671.
- [2] F. Neese, *Wires Comput Mol Sci* **2012**, *2*, 73-78.
- [3] J. G. Brandenburg, C. Bannwarth, A. Hansen, S. Grimme, *Journal of Chemical Physics* **2018**, *148*.
- [4] T. Lu, F. W. Chen, *Journal of Computational Chemistry* **2012**, *33*, 580-592.
- [5] J. Zhang, T. Lu, *Phys Chem Chem Phys* **2021**, *23*, 20323-20328.
- [6] J. M. Wang, R. M. Wolf, J. W. Caldwell, P. A. Kollman, D. A. Case, *Journal of Computational Chemistry* **2004**, *25*, 1157-1174.
- [7] Pekka Mark, Lennart Nilsson, *J. Phys. Chem. A*, **2001**, *43*: 105.
- [8] Abraham, M.J, Murtola, T, Schulz, R., *SoftwareX*, **2015**, *1*, 19.
- [9] Jen H, Anton A, Ying Y, *Curr. Protoc. Bioinformatics*, **2008**, *5*: 7.